

# PARACONDUCTIVITY OF (Bi,Pb)<sub>2</sub>Sr<sub>2</sub>Ca<sub>2</sub>Cu<sub>3-x</sub>Ge<sub>x</sub>O<sub>y</sub>

R. K. NKUM, BSc, MSc, DSc CPhys MInstP  
DEPARTMENT OF PHYSICS  
UNIVERSITY OF SCIENCE AND TECHNOLOGY - KUMASI, GHANA.

## ABSTRACT

The paraconductivity of (Bi,Pb)<sub>2</sub>Sr<sub>2</sub>Ca<sub>2</sub>Cu<sub>3-x</sub>Ge<sub>x</sub>O<sub>y</sub> (0 ≤ x ≤ 0.3) superconducting system has been investigated. The paraconductivity above T<sub>c</sub> was determined from the Anderson-Zou fit to the normal-state resistivity. Using the Aslamazov-Larkin theory, the dimensionality of the materials was determined. The value of the critical exponent (λ-1) obtained for all the samples indicates that the superconductivity of the system in which Ge replaces Cu is of two-dimensional nature. Thus, the substitution of Ge for Cu does not affect the homogeneity in the superconducting fluctuations in the Cu-O planes. There is evidence that the a-b plane conductivity dominates, although the crystallites in the polycrystalline samples are randomly oriented.

**KEYWORDS:** superconductivity, paraconductivity, fluctuations, dimensionality

## INTRODUCTION

One of the properties which have mostly been used to characterise superconductors is the electrical resistivity. Indeed, a superconductor is basically a material whose electrical resistivity becomes zero at a certain critical temperature. The linear temperature behaviour of the electrical resistivity at high temperatures was one of the first observations of the high temperature superconductors. This is not yet fully understood. Interpretations of linear ρ(T) so far range from a most conventional electron-phonon scattering model to a most exotic resonating valence bond model.

Above the transition temperature, T<sub>c</sub>, thermal fluctuations of the order parameter deviating from the Ginzburg-Landau equilibrium value in superconductors occur. This means that small regions of the superconductor fluctuate in the superconducting state. The additional conductivity due to these fluctuations is called "paraconductivity" or excess conductivity. The study of the temperature dependence of the paraconductivity is a way to check the dimensionality of the fluctuations in the order parameter and therefore the dimensionality of the superconducting properties. These fluctuations give rise to a rounding of the ρ(T) curve above T<sub>c</sub>. But because the characteristic coherence length in the classical superconductors is quite large the thermodynamic fluctuations are usually small except for a narrow temperature

interval. For this reason in the classical superconductors the paraconductivity is usually experimentally accessible only for samples with reduced Euclidean dimensionality (e.g. films, filaments). In this case the temperature region where the paraconductivity is reasonably large is somewhat broader because of the higher absolute values of the critical exponents.

In the case of the high temperature superconductors the coherence length is a very small. The small coherence length gives a small coherence volume which contains only a few Cooper pairs. This implies that fluctuation would play a much larger role in these materials than in the conventional superconductors.

The paraconductivity Δσ is defined as

$$\Delta\sigma = \sigma(T) - \sigma_N(T) \quad (1)$$

where σ<sub>N</sub>(T) is the background normal-state conductivity and σ(T) is the measured conductivity. Taking into account the direct influence of the thermal fluctuations above T<sub>c</sub>, Aslamazov and Larkin (AL) derived an expression for the paraconductivity [1].

$$\Delta\sigma/\sigma_{300K} = A\epsilon^\lambda, \quad (2)$$

where A is temperature-independent amplitude, λ is a critical exponent, ε = (T - T<sub>c</sub>)/T<sub>c</sub>, and σ<sub>300K</sub> is the normal-state conductivity at 300K. Both A and λ depend strongly on the superconducting dimensionality and coherence length. Thus, the analysis of the paraconductivity gives valuable information of the dimensionality and the coherence length of the system.

The coherence length sets the length scale for the variation of the superconducting order parameter. The small value of the coherence length of the high temperature superconductors, therefore, implies that the superconductivity will be more sensitive to small structural or chemical imperfections than in a conventional superconductor. Recently, Nkum and Datar [2] and Nkum [3] have investigated the effect of Sn on the inhomogeneous character and the induced fluctuation of superconductivity in the Bi-based system. Sn-substitution for Cu was found to cause spatial disorder in the Cu-O<sub>2</sub> planes which breaks the homogeneity of the superconducting fluctuations in these planes. This gives motivation for further work to be done on the effect of impurities on the superconducting fluctuations in the oxide superconductors.

In this work, the results of measurements and analysis of the paraconductivity of the 2223 phase of Ge substitution for Cu in the Bi-Pb-Sr-Ca-Cu-O system are presented and discussed.

## EXPERIMENTAL METHOD

Details of the conditions of preparation of the samples with the nominal composition Bi<sub>1.6</sub>Pb<sub>0.4</sub>Sr<sub>2</sub>Ca<sub>2</sub>Cu<sub>3-x</sub>Ge<sub>x</sub>O<sub>y</sub> (0 ≤ x ≤ 0.3) are reported elsewhere [4].

The electrical resistivities of the samples were measured in the temperature range 50 - 300 K by the standard four-probe technique. The 50 K temperature was obtained by pumping in liquid nitrogen. The contact areas of the rectangular shaped samples were painted with silver paste. The samples

were then annealed at 600°C for 30 min. and slowly cooled to room temperature. The electrodes were formed by four fine copper wires (14 μm diameter) which were affixed to the fired contact areas with the same paste. This procedure ensures low contact resistances which were of the order of 0.3Ω for a contact area of 0.1 mm<sup>2</sup> in the superconducting state. Temperatures were measured to an accuracy of 0.1 K with a platinum resistance thermometer. At each temperature the voltage readings were taken for both forward and reverse directions of current flow to correct for any thermo-emfs at the contacts. Current of 1 mA was used for all samples.

## RESULTS AND DISCUSSION

Figure 1 shows the temperature dependence of the electrical resistivity of the samples. There is a linear temperature dependence for the temperatures above 150 K. The resistivity deviates from linearity below 150 K with a rounding off slightly above  $T_c$ .

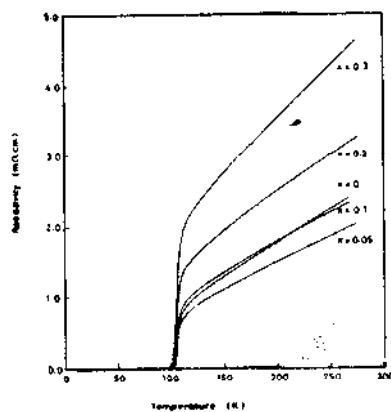


Figure 1

The choice of the transition temperature,  $T_c$ , plays a significant role in the evaluation of the paraconductivity. In this work,  $T_c$  is defined as the temperature at which  $d\rho/dT$  versus  $T$  shows a maximum, or  $\rho$  versus  $T$  has its inflection point. A representative  $d\rho/dT$  versus  $T$  curve is given in Fig. 2

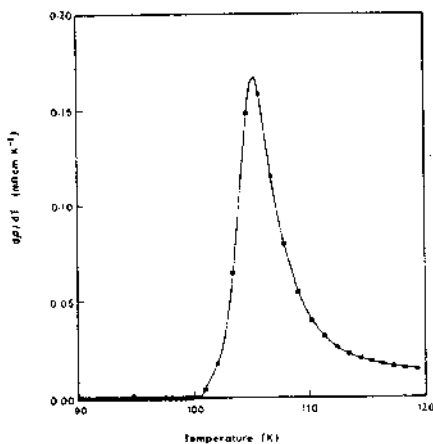


Figure 2

for the  $x=0$  sample. The temperature derivative is numerically determined by a third-order polynomial fit to seven points. The values of  $T_c$  for the samples are given in Table 1. The transition widths of the samples, determined at the half-maximum of the  $d\rho/dT$  curves, are given in Table 1. The width of the transition is presumably related to the distribution of  $T_c$  among the grains.

Table 1: Some resistivity parameters of  $\text{Bi}_{1-x}\text{Pb}_x\text{Sr}_2\text{Ca}_2\text{Cu}_3\text{Ge}_4\text{O}_{10}$

Sample x	AZ fit				
	$T_c$ (K)	$\Delta T$ (K)	$a$ (mΩ cm/K)	$b$ (μΩ m/K)	$\lambda$
0	106.8	4.0	1.550	8.995	-1.005
0.05	105.6	4.7	9.253	7.276	-1.010
0.10	104.5	6.0	30.432	8.275	-0.995
0.20	105.0	6.7	58.405	11.057	-0.997
0.30	106.4	6.8	70.670	15.973	-1.028

Anderson and Zou [5] have proposed an interesting mechanism for the current transport between adjacent Cu-O planes. In the resonant-valence-bound theory, conduction in the normal state is mediated by holons (hole bosons) which are confined to each Cu-O plane. Tunnelling between the planes is only possible for real electrons which can be formed by merging the two types of soliton-like excitations of the two-dimensional (2D) Cu-O planes, namely, the holon (spin 0, charge 1) with the spinon (spin 1/2, charge 0). As expected for a scattering of bosons by fermions, the temperature dependence of the a-b plane resistivity,  $\rho_{ab}$ , is linear in  $T$ . The probability of a tunnelling process between the planes is proportional to the spinon density which is linear in  $T$ , leading to a resistivity  $\rho_c \sim 1/T$ . Accordingly, the normal-state resistivity in both the a-b plane and the c direction is given by

$$\rho(T) = a/T + bT \quad (3)$$

where the hyperbolic term is introduced to model the interplane hopping of carriers. Since the samples under study are polycrystalline, the resistivity measured is the average for the a-b plane and the c direction. Thus eq. (3) is a good representation of the resistivity in the ceramic system.

Anderson-Zou model is used in this study by plotting the product  $\rho T$  versus  $T^2$  in Fig. 3. The samples fulfil the predicted temperature dependence of the resistivity as indicated by the straight lines in Fig. 3. The excess conductivity was determined from this model. The values of the constants  $a$  and  $b$  (Eq. (3)) determined from the linear plot are listed in Table 1. These values are in good agreement with those found for other Bi-based systems [3] and those found by Anderson and Zou [5] using single crystal data. This implies that the resistivity behaviour in dense, high quality polycrystalline materials is intrinsic to single grain and thus similar to that of  $\rho_{ab}$  in single crystals.

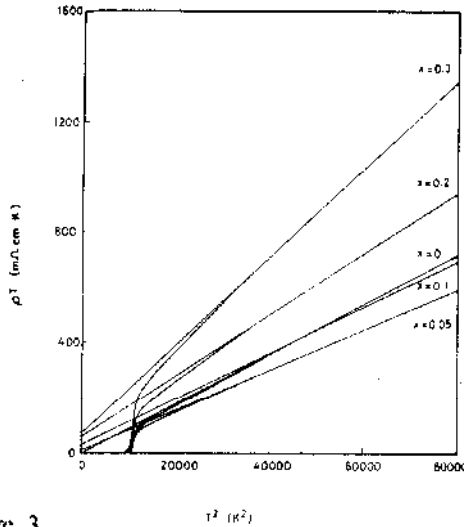


Figure 3

The normalised excess conductivity,  $(\Delta\sigma/\sigma_{300K})$ , is plotted against the reduced temperature. Figure 4 shows the plot for the  $x=0.1$  sample. The  $\ln(\Delta\sigma/\sigma_{300K})$  versus  $\ln\xi$  plot is reasonably linear over a wide range of  $\ln\xi$ . The critical exponents obtained for these regions for the samples are given in Table 1. The value of the critical exponent obtained for the samples indicate a 2D superconductivity in the samples. Thus, unlike Sn-substitution which was found to affect the dimensionality of the 2223 Bi-based system, Ge-substitution has no such effect. This means that replacement of some Cu atoms by Ge does not affect the homogeneity of the superconducting fluctuations in the Cu-O planes. The dimensionality is two for both the Ge-free and the Ge-substituted samples.

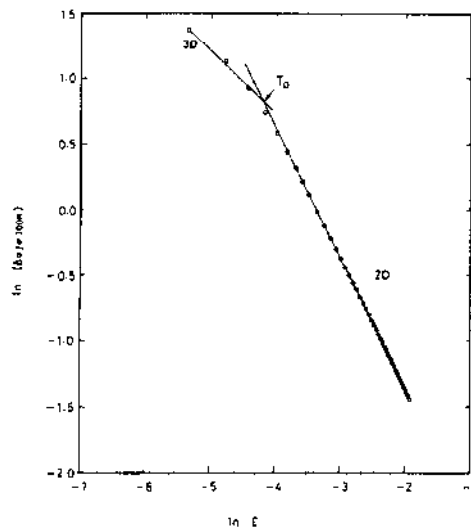


Figure 4

Results of the measurements of resistivity of single crystals of both Y-Ba-Cu-O and Bi-Sr-Ca-Cu-O show that the a-b plane resistivity is lower in magnitude than the c direction resistivity [6,7]. The a-b-plane resistivity, which according to the Anderson-Zou model varies linearly with temperature, therefore, dominates in a parallel circuit network. The fit of the Anderson-Zou model indicates that although the polycrystalline samples consist of randomly oriented crystallites, due to very high anisotropy, the a-b plane resistivity dominates in the equivalent parallel resistor network. The resistivity of the polycrystalline samples, then, has the same behaviour, and hence yields the same type of information as does  $\rho_{ab}$  in a single crystal study.

The two contributions of the paraconductivity  $\Delta\sigma$  are the direct contribution which results from the acceleration of superconducting pairs and the indirect contribution due to the interaction of superconducting fluctuations with the normal electrons. Neglecting the indirect contribution, Lawrence and Doniach [8] calculated the paraconductivity parallel to the layers in a superconducting compound:

$$\Delta\sigma = e^2/16\hbar e \{1 + [2\xi_c(0)/d]^2 \epsilon^{-1}\}^{-0.5} \quad (4)$$

For temperatures close to the BSC mean-field transition, the ratio  $2\xi_c(T)/d \gg 1$  and  $\Delta\sigma$  diverges as  $\epsilon^{-1/2}$  which corresponds to the three-dimensions (3D) behaviour. For temperatures  $T > T_c$  the ratio  $2\xi_c(T)/d \ll 1$  and  $\Delta\sigma$  diverges as  $\epsilon^{-1}$  (2D behaviour). Due to the very short coherence length  $\xi_c(0)$  the dimensionality crossover temperature

$$T_c = T_c \{1 + [2\xi_c(0)/d]^2\} \quad (5)$$

is expected to be close to  $T_c$  in a temperature range where  $\Delta\sigma$  is still measurable.

From Eq.(2), the amplitude for a 2D system is

$$A = (e^2\rho_{300K})/16\hbar d \quad (6)$$

where  $\rho_{300K}$  is the normal-state resistivity at 300 K and  $d$  is the thickness of the superconducting layer. The value of  $d$  could be determined from the plot of  $\ln(\Delta\sigma/\sigma_{300K})$  versus  $\ln\xi$  (from Eq.(2)) and Eq. (6).  $T_c$  was obtained as shown in Fig.4. Close to the transition temperature, there is a crossover from 2D to 3D, as expected for layered system [8]. Using the values of  $T_c$ ,  $T_c^*$ ,  $d$  and Eq.(5) the coherence lengths of the samples were calculated. The results are indicated in Fig.5. It can be seen from Fig.5 that the coherence length is sample dependent. This indicated clearly that the coherence length is dependent on the inhomogeneities that also affect the normal-state electrical conductivity.

In general, inhomogeneity reduces the coherence length of a superconducting system (as seen for  $x=0.05$ ) since the introduction of impurities reduces the thickness of the superconducting layer. However, the effect of impurities may not be the same for the a-b plane and c directions in a polycrystalline sample due to the anisotropic nature of the Bi-based system. Measurement of the critical fields in  $\text{Bi}_2\text{Sr}_2\text{Ca}_1\text{Cu}_2\text{O}_x$  single crystals [9] gave coherence lengths of  $30.1\text{\AA}$  in the a-b plane and  $5.7\text{\AA}$  in the c direction. The difference in the coherence lengths in the two directions is due to the large anisotropy of these materials. The values obtained

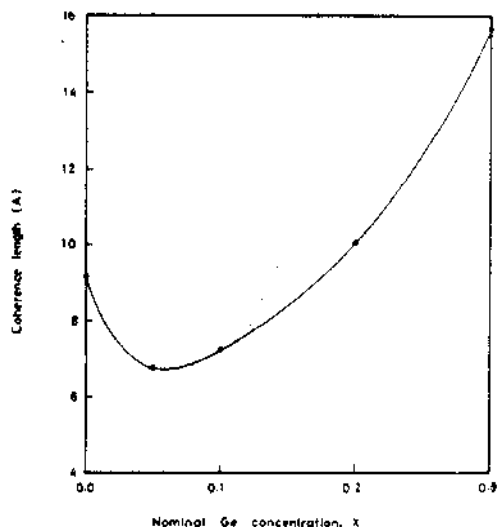


Figure 5

for the samples under study in this work are the polycrystalline average and agree well with the values obtained by Nkum and Datars [2,10]. It is possible that more Ge atoms ( $x > 0.1$ ) enhance the growth of superconducting crystallites with orientation in the a-b plane more than in the c direction. This could explain the increase in the coherence length for the  $x = 0.1$  samples after an initial drop for the  $x = 0.05$  sample. This model is in agreement with the excellent fit of the  $(T_c)$  curve with the Anderson-Zou relation.

## CONCLUSION

The Anderson-Zou model has been used to determine the paraconductivity above the transition temperature. The paraconductivity from the superconducting fluctuations shows a power law behaviour with a critical exponent  $\lambda$ . The values of the critical exponent obtained from the experimental excess conductivity clearly indicate that superconductivity in the  $(\text{Bi,Pb})_2\text{Sr}_2\text{Ca}_2\text{Cu}_{1-x}\text{Ge}_x\text{O}_y$  system is of two-dimensional nature. Thus, unlike Sn, the substitution of Ge for Cu does not break the homogeneity in the superconducting fluctuations in the Cu-O planes. Very close to  $T_c$ , a crossover to 3D is observed. The coherence length observed for the samples agree quite well with published values of Bi-based polycrystalline superconductors. The coherence length is, however, sample dependent. The excellent fit of the Anderson-Zou model indicates that although the crystallites in the polycrystalline samples are randomly oriented, the conductivity in the a-b plane dominates.

## Acknowledgement:

I am grateful to all my colleagues for their encouragement. I acknowledge the use of the facilities of the Department of physics.

## REFERENCES

1. Aslamazov, L.G., and Larkin, A.I., *Effect of Fluctuations on the Properties of a Superconductor Above the Critical Temperature. Sov.Phys. - Solid State* **10**: 875-879, 1968.
2. Nkum, R.K., and Datars, W.R., *Fluctuation Induced Conductivity in the Sn-doped  $(\text{Bi,Pb})_2\text{Sr}_2\text{Ca}_2\text{Cu}_x\text{O}_y$  Superconducting system. Physica C* **192**: 215-222, 1992
3. Nkum, R.K., *Resistive Transition in the Sn-doped  $(\text{Bi,Pb})_2\text{Sr}_2\text{Ca}_2\text{Cu}_x\text{O}_y$  Ceramic System: Percolation and Fractal Behaviour. Submitted to Turkish Journal of Physics.*
4. Nkum, R.K., and Datars, W.R., *Superconductivity in a Ge-doped Bi-Pb-Sr-Ca-Cu-O System. Supercond. Sci. Technol.* **5**: 549-555, 1992
5. Anderson, P.W., and Zou, Z., *Phys. Rev. Lett.* **60**: 132, 1988.
6. Chandrasekhar, M.R., Mulla, I.S., and Sinha, A.P.B., *Appl. Phys. Lett.* **55**: 1472, 1989
7. Briceno, G., Crommie, M.F., and Zetti, A., *Phys. Rev. Lett.* **66**: 2164, 1991.
8. Lawrence, W.E. and Doniach, S., *In: Proceedings of the XII International Conference on Low temperature Physics, Kyoto, 1970, edited by E. Kanda (Keigaku, Tokyo, P. 361), 1971.*
9. Mandal, P., Poddar, A., Das, A.N., Ghosh, B., and Choudhury, P., *Excess Conductivity and Thermally Activated Dissipation Studies in  $\text{Bi}_2\text{Sr}_2\text{Ca}_2\text{Cu}_x\text{O}_y$  Single Crystals. Physica C* **169**: 43-49, 1990
10. Nkum, R.K., and Datars, W.R., *Fluctuation-enhanced Conductivity in the Sn-doped Bi-Pb-Sr-Ca-Cu-O Superconducting System. Phys. Rev. B* **44**: 12516-12520, 1991.

## Figure Caption

Figure 1: Temperature dependence of the electrical resistivity of  $\text{Bi}_{1.6}\text{Pb}_{0.4}\text{Sr}_2\text{Ca}_2\text{Cu}_{1-x}\text{Ge}_x\text{O}_y$

Figure 2: Temperature dependence of the temperature derivative of the electrical resistivity of  $\text{Bi}_{1.6}\text{Pb}_{0.4}\text{Sr}_2\text{Ca}_2\text{Cu}_x\text{O}_y$ . The temperature at which the peak occurs is taken as  $T_c$ .

Figure 3: The Anderson-Zou plot of the resistivity-temperature data of Fig. 1

Figure 4: Log-log plot of the excess conductivity above  $T_c$  versus reduced temperature for  $\text{Bi}_{1.6}\text{Pb}_{0.4}\text{Sr}_2\text{Ca}_2\text{Cu}_x\text{O}_y$ .  $T_c$  is the 2D-3D crossover temperature.

Figure 5: The dependence of the coherence length of  $\text{Bi}_{1.6}\text{Pb}_{0.4}\text{Sr}_2\text{Ca}_2\text{Cu}_{1-x}\text{Ge}_x\text{O}_y$  on the normal-state resistivity at 300 K.

# MONITORING OF NATURAL BACKGROUND RADIATION IN SOME GHANAIAN HOMES

O.C. OPPON, BSc, DU  
 H.M. ANIAGYEI, DIP ENG MSc  
 A.W.K. KYERE, BSc MSc PhD  
 NATIONAL NUCLEAR RESEARCH INSTITUTE, ACCRA, GHANA

## ABSTRACT

*The high incidence of cancer amongst people residing in certain specific regions in the world has given rise to the need to monitor the natural background radiation exposure. The major contributor to this background radiation is Rn-222 and its daughters. In Ghana an attempt is on the way to map out regions of high natural background radiation through the monitoring of radon gas in homes. Two main types of construction techniques are used in Ghana. These are the modern house constructed mainly from cement blocks and the traditional house built from sun-baked mud blocks. These measurements were carried out using alpha sensitive track detector LR115, and the counting done using a spark counter. The results are presented in this paper.*

**KEYWORDS:** Background dose, radon gas, track detectors, spark counter.

## INTRODUCTION

Natural radiation is contributed mainly from two sources; cosmic and terrestrial. For the terrestrial sources the major contributor is uranium bearing materials ever present in the soil. Uranium-238 decays through a series to produce Ra-226, and subsequently Rn-222 gas with a half life of 3.82 days, and finally ending as Pb-206. The high concentration of radon gas which can occur in enclosed environments and its subsequent decay is known to be a major contributor to high levels of natural radiation to which populations are exposed. There is therefore, the risk of cancer induction amongst such populations [1].

In sub-saharan Africa, little information is available on the average exposure to which people in this region are subjected to from this source of natural radiation indoors. A pilot study is being carried out in Ghana to study this exposure by measuring the radon concentrations in both traditional houses and those built with modern technology.

The traditional houses are constructed with mud bricks made from clay deposits available at the site of construction. These houses have, in most cases, only small single windows for ventilation and therefore correspondingly small air exchange rates. The modern houses are constructed

from sandcrete blocks with an average of about two large windows per room and therefore have high air exchange rates.

The area selected for this monitoring was Dome village near the National Nuclear Research Institute and some houses at the residential area of some of the staff of the institute. The radiation dose received by each group of dwellings has been estimated from the average radon concentration measured.

## METHOD

The radon gas measurements for these houses were done for the traditionally constructed houses during nine month period, i.e. 7th March 1989 to 7th December 1989, at three monthly intervals. However, one test house in Dome village was monitored continuously for one year from September 1989 to September 1990.

Due to the suspected low levels of radon gas in the modern houses, a single seven month period of exposure from February 1990 to September 1990 was adopted. Nine single unit houses, two storey buildings and two blocks of three storey flats were monitored. The flats had two bedrooms, a living room, a kitchen and bathroom on the same floor while the rest of the units had three bedrooms each with similar amenities all under one roof. Twenty-five houses were monitored at the village. These houses were mostly single bedrooms with the other amenities situated some distance away from the main building. After exposure the LR115 foils were etched; in 2.5M NaOH at 60°C for 110 minutes. The counting of the tracks was done using a spark counter. The calibration of the dosimeters was done by comparison with the bare LR115 detector whose calibration factor for radon measurement was known [2,3].

## RESULTS AND DISCUSSION

The lower limit of detection (LLD) for the radon measurement system was calculated from Currie [4], using a measured background track density uncertainty of 3/cm<sup>2</sup> and an area counted of 1.766 cm<sup>2</sup>. The LLD was 5 Bq/m<sup>3</sup> and 2 Bq/m<sup>3</sup> for the 3 months period and 7 months period respectively.

The average radon concentration for the modern sandcrete building was found to be 2 Bq/m<sup>3</sup>. This is at the threshold of detection for the seven months exposure period. The mean for the nine single unit houses was 3 Bq/m<sup>3</sup> which was the same for the one storey buildings. The fourth storeys of the block of flats had an average value of 1.0 Bq/m<sup>3</sup>. This shows the thinning out of radon concentration with height above the ground level.

For the traditionally constructed houses, the mean



Dr. O.C. Oppon



Mr. H.N. Aniagyei



Dr. A.W.K. Kyere

radon concentration was  $121 \text{ Bq/m}^3$  with a standard error of the mean being  $15 \text{ Bq/m}^3$  for all the measurements during the nine months exposure period. The test house monitored continuously for a year period had a mean value of  $28 \text{ Bq/m}^3$ .

During the period from March to June, nine houses exceeded the remedial action limit of  $150 \text{ Bq/m}^3$  with three of these exceeding the immediate action level of  $400 \text{ Bq/m}^3$  set by the Environmental Protection Agency (EPA) of the United States [5]. The mean for this period was  $171 \pm 34 \text{ Bq/m}^3$ . The radon concentrations range from below  $5 \text{ Bq/m}^3$  to  $580 \text{ Bq/m}^3$ .

For the period June to September the mean radon concentration was  $96 \pm 16 \text{ Bq/m}^3$ . The range of radon concentration was between  $5 \text{ Bq/m}^3$  and  $336 \text{ Bq/m}^3$  with the concentration in four houses exceeding the remedial action level. The period from September to December had a mean radon concentration of  $62 \text{ Bq/m}^3$  with a range from  $5 \text{ Bq/m}^3$  to  $325 \text{ Bq/m}^3$ . Three houses exceeded the remedial action level. The changes in the three monthly mean values reflect the weather changes during the period from March to late July when there are rains with accompanying colder nights. The rest of the year is normally dry with warmer nights.

The radon concentration distribution for the two measurement periods are shown in Fig. 1. The skew is towards the lower radon concentration. The range  $0.49 \text{ Bq/m}^3$  constitutes 55% of the total with 38% of this range being due to the sandcrete houses at the residential area of the Institute.

The radon dose calculations are based on the dose conversion coefficient now being recommended by the ICRP that an exposure to  $20 \text{ Bq/m}^3$  of radon gas in typical indoor conditions will give rise to an effective equivalent dose of  $1 \text{ mSv/yr}$  [6]. Based on this the radiation dose due to the radon concentration in the so called modern houses was  $0.1 \text{ mSv/yr}$ . For the traditionally constructed houses the average dose was  $6 \text{ mSv/yr}$ , with a dose range of  $0.35$  to  $17 \text{ mSv/yr}$ . The dose received in the test house monitored for a one year period was  $1.4 \text{ mSv/yr}$ . The occupancy factor for the village dwellings is about 8 hours per day as the rooms serve mainly as sleeping places. The factor for the modern house is on the average 14 hours per day due to the provision of all the basic necessities under one roof.

Taking these factors into consideration the dose received by the occupant would be  $0.06 \text{ mSv/yr}$  for the modern house dweller and  $2.0 \text{ mSv/yr}$  for the village house dweller. The natural background radiation dose due to radon is lower in the sandcrete houses than mud houses. This can be attributed mainly to the ventilation rates.

## CONCLUSION

These results are an attempt to quantify the radon concentration and its dose contribution due to the natural background radiation in modern and traditionally constructed houses in Ghana. Since this is a pilot study the sample size is small but these modes of construction are predominantly the same for the West African Sub-region. These results can therefore be the basis upon which future comparisons can be made. The study would be extended when the logistics are available to cover a larger population.

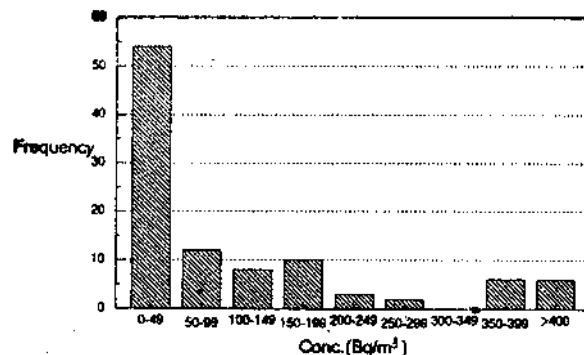


Fig. 1 Radon Concentration Distribution for some Ghanaian Homes

## ACKNOWLEDGEMENTS

The authors appreciate the efforts of Mr F. B. Johnson for his assistance with the difficult task of convincing the village dwellers to accept the dosimeters in their homes and also with the processing of the detectors. The authors also wish to thank the International Atomic Agency for financing the project.

## REFERENCES

1. **BEIR REPORTS.**  
*Health Risk of Radon and other Internally deposited alpha-emitters. No. iv, pp 5-9, 1988.*
2. **Oppon, O.C.,**  
*Bare Detectors for short-term Measurements Workshop on Radon Monitoring in Radioprotection, Environmental Radioactivity and Earth Sciences. pp 171-176, April 1989.*
3. **Rannou, A., Jeanmarie, L. et al.**  
*Use of Cellulose Nitrate as Radon and Radon Daughter Detector for Indoor Measurements. Nuclear Tracks No. 12, pp 747-750, 1986*
4. **Nelson, R.A.**  
*Measurement Uncertainties of Long term Rn-222 average at environmental levels using alpha track Detectors. Health Physics No. 40, pp 693-702, 1987.*
5. **US-EPA Report.**  
*A Citizen's Guide to Radon. No. OPA-86-004. N.C. USA 1986*
6. **Poitr Wasiolek.**  
*Radon Exposure Physics Bulletin No. 10P, pp. 143-144, 1988*